
SUCHST DU NOCH ODER LIEST DU SCHON?

Wie bringt man einem Computer Zukunftsforschung bei?



Dr. Marcus John

Tag der Offenen Tür

8. Juli 2017

Fraunhofer INT

Euskirchen



Wie bezahlen wir
in Zukunft im Laden?

Woraus werden Pumpen
im Jahre 2030 gebaut?

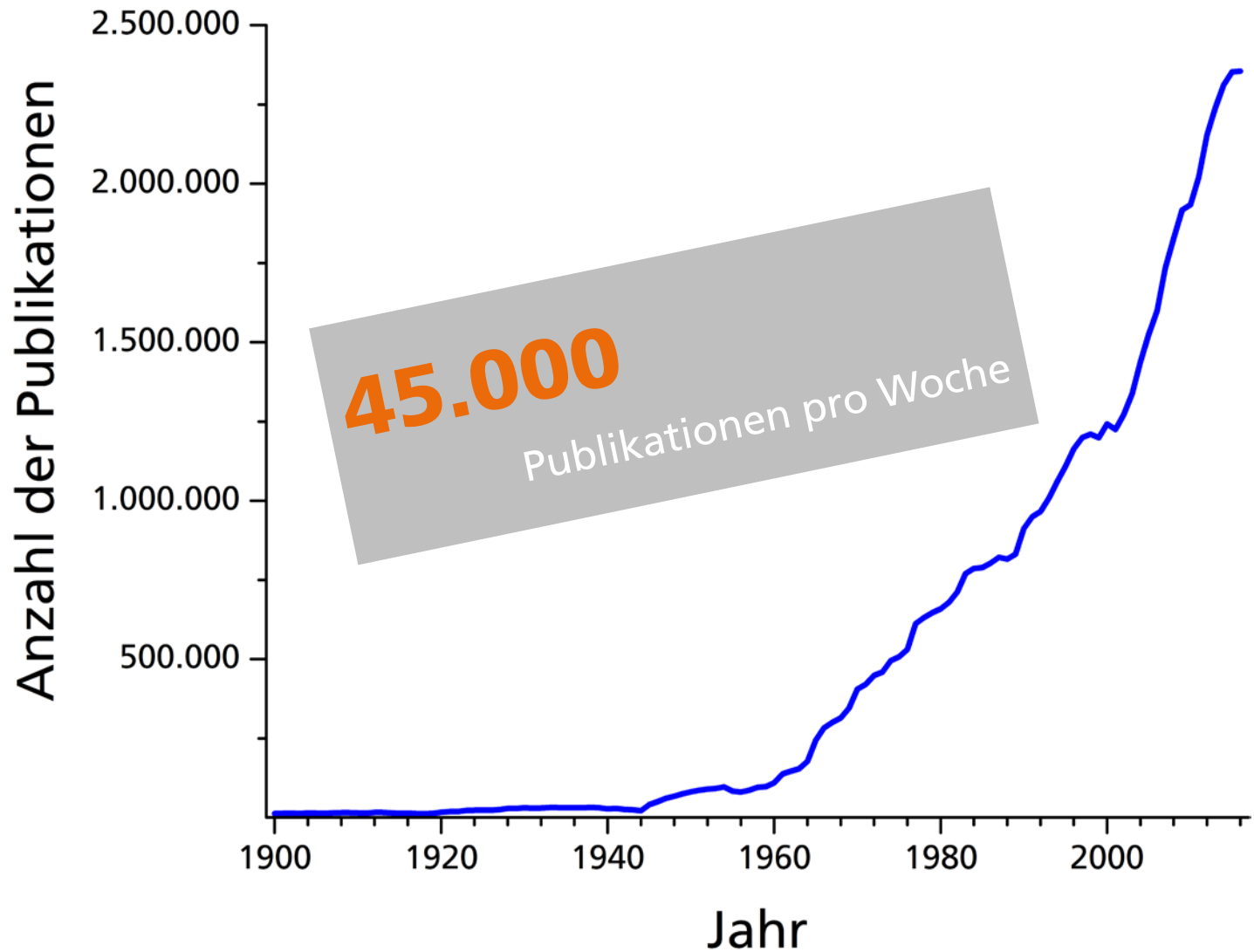
Können wir den
Menschen
leistungsfähiger machen?

Werden wir 2035 noch
Waschmaschinen haben?

Wir benötigen eine Art


Science Observatory

Mehr als **2.300.000** Publikationen 2016



← Comparing single-particle analysis data of volcanic ash of the 2010 Eyjafjallajökull eruption obtained from scanning electron and light microscope images

Frank Sommer, Christoph Maschowski, Volker Dietze, Bernard Grobéty, Reto Gieré

DOI: 10.1127/ejm/2016/0028-2555  Published on December 2016, First Published on June 08, 2016

[Article](#)[Figures](#)[Info & Metrics](#)

© 2016 E. Schweizerbart'sche Verlagsbuchhandlung Science Publishers

Abstract

This study examines the influence of different analysis techniques on the results concerning the particle size distribution and mineralogical composition of airborne particles. Volcanic ash from the Eyjafjalla volcano was examined with a transmitted light microscope (TLM), a scanning electron microscope (SEM), SEM equipped with an automatic single-particle analysis program, and an electron microprobe (EMP) and the results differ considerably. Main error source is the specific particle analysis method. Here, a sample containing airborne particles of volcanic material was analysed with the different methods on the evaluation area per unit time (number settling rate). The results obtained by manual SEM and EMP analysis with

BRIEF REPORT

Zika Virus Associated with Microcephaly

Jernej Mlakar, M.D., Misa Korva, Ph.D., Nataša Tul, M.D., Ph.D.,
Mara Popović, M.D., Ph.D., Mateja Poljšak-Prijatelj, Ph.D., Jerica Mraz, M.Sc.,
Marko Kolenc, M.Sc., Katarina Resman Rus, M.Sc., Tina Vesnaver Vipotnik, M.D.,
Vesna Fabjan Vodušek, M.D., Alenka Vizjak, Ph.D., Jože Pižem, M.D., Ph.D.,
Miroslav Petrovec, M.D., Ph.D., and Tatjana Avšič Županc, Ph.D.

SUMMARY

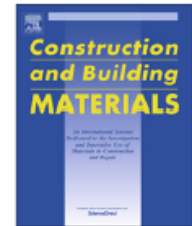
A widespread epidemic of Zika virus (ZIKV) infection was reported in 2015 in South and Central America and the Caribbean. A major concern associated with this infection is the apparent increased incidence of microcephaly in fetuses born to mothers infected with ZIKV. In this report, we describe the case of an expectant mother who had a febrile illness with rash at the end of the first trimester of pregnancy while she was living in Brazil. Ultrasonography performed at 29 weeks of gestation revealed microcephaly with calcifications in the fetal brain and placenta. After the mother requested termination of the pregnancy, a cesarean section was performed. Micrencephaly (an abnormally small brain) was diagnosed, with almost complete agyria, hydrocephalus, and multifocal calcifications in the cortex and subcortical white matter, with associated multifocal microglial and focal inflammation. ZIKV was detected in the placenta and fetal brain.



Contents lists available at [ScienceDirect](#)

Construction and Building Materials

journal homepage: www.elsevier.com/locate/conbuildmat



Air pollutant emissions and acoustic performance of hot mix asphalts



Lin Shiyong*, Hung Wingtat, Leng Zhen

The Department of Civil and Environmental Engineering, The Hong Kong Polytechnic University, Hong Kong

HIGHLIGHTS

- Temperature has a great effect on gaseous and particulate emissions.
- Total PAHs observed is still far below the specified limitation.
- The PM_{2.5} variations on the construction site can be significant.
- VOC concentrations are in general extremely low from the laboratory and the field.
- The PMSMA6 shows the best low noise performance among the other tested surface types.

ARTICLE INFO

ABSTRACT

This paper



ELSEVIER

Contents lists available at ScienceDirect

Journal of Alloys and Compounds

journal homepage: <http://www.elsevier.com/locate/jalcom>



Magnetic/structural phase diagram and zero temperature coefficient of resistivity in $\text{GaFe}_{3-x}\text{Co}_x$ ($0 \leq x \leq 3.0$)



X.C. Kan^{a, b}, B.S. Wang^{a, *}, S. Lin^a, B. Yuan^a, L. Zu^{a, b}, X.F. Wang^{a, b}, J.C. Lin^a, P. Tong^a,
W.H. Song^{a, *}, Y.P. Sun^{c, a, d}

^a Key Laboratory of Materials Physics, Institute of Solid State Physics, Chinese Academy of Sciences, Hefei 230031, China

^b University of Science and Technology of China, Hefei 230026, China

^c High Magnetic Field Laboratory, Chinese Academy of Sciences, Hefei 230031, China

^d Collaborative Innovation Center of Advanced Microstructures, Nanjing University, Nanjing 210093, China

ARTICLE INFO

Article history:

Received 28 April 2015

Received in revised form

16 December 2015

Accepted 20 December 2015

Available online 23 December 2015

Keywords:

Magnetic/structural phase diagram

ABSTRACT

Magnetic/structural phase diagram of $\text{GaFe}_{3-x}\text{Co}_x$ ($0 \leq x \leq 3.0$) were investigated systematically. It was found that the antiperovskite phase collapses at $x = 0.90$ and recovers again at $x = 2.3$ with Co doping. Along with this transformation, the ferromagnetic state in GaFe_3 is suppressed and a reentrant spin-glass state ($2.3 \leq x \leq 2.6$) or enhanced magnetic reorientation is observed. The temperature dependence of the magnetic susceptibility and magnetic relaxation were adopted to study the origin of the collapsed antiperovskite phase. It is concluded that the contractive lattice as well as the magnetic reorientation is the origin of the collapsed antiperovskite phase. The magnetic reorientation is achieved by Co-doping and the magnetic reorientation is suppressed at low temperature.

Exploiting Weak PUFs From Data Converter Nonlinearity—E.g., A Multibit CT $\Delta\Sigma$ Modulator

Andreas Herkle, *Student Member, IEEE*, Joachim Becker, *Member, IEEE*, and Maurits Ortmanns, *Senior Member, IEEE*

Abstract—This paper presents a novel approach of deriving physical unclonable functions (PUF) from correction circuits measuring and digitizing nonlinearities of data converters. The often digitally available correction data can then be used to generate a fingerprint of the chip. The general concept is presented and then specifically evaluated on an existing Delta-Sigma ($\Delta\Sigma$) modulator whose outermost feedback DAC mismatches are greatly influencing the overall performance and thus need correction. The applied mixed-signal correction scheme reveals the intrinsic mismatches which are firstly used to linearize the $\Delta\Sigma$ modulator, but can also be further analyzed. The intra-Harmonic

equally weighted unit elements as they introduce differential nonlinearities (DNL) which reduce the effective resolution of the conversion result [4]. While the influence of a single mismatching unit element might be small enough to be neglected, the summed up output of many elements in a data converter results in an integral nonlinearity (INL) which significantly decreases the effective resolution. Moreover,

Planck 2015 results

XIII. Cosmological parameters

Planck Collaboration: P. A. R. Ade¹⁰⁵, N. Aghanim⁷¹, M. Arnaud⁸⁷, M. Ashdown^{83,7}, J. Aumont⁷¹, C. Baccigalupi¹⁰³, A. J. Banday^{117,12}, R. B. Barreiro⁷⁸, J. G. Bartlett^{1,80}, N. Bartolo^{38,79}, E. Battaner^{120,121}, R. Battye⁸¹, K. Benabed^{72,116}, A. Benoit⁶⁹, A. Benoit-Lévy^{29,72,116}, J.-P. Bernard^{117,12}, M. Bersanelli^{41,58}, P. Bielewicz^{97,12,103}, J. J. Bock^{80,14}, A. Bonaldi⁸¹, L. Bonavera⁷⁸, J. R. Bond¹¹, J. Borrill^{17,109}, F. R. Bouchet^{72,107}, F. Boulanger⁷¹, M. Bucher¹, C. Burigana^{57,39,59}, R. C. Butler⁵⁷, E. Calabrese¹¹², J.-F. Cardoso^{88,1,72}, A. Catalano^{89,86}, A. Challinor^{75,83,15}, A. Chamballu^{87,19,71}, R.-R. Chary⁶⁸, H. C. Chiang^{33,8}, J. Chluba^{28,83}, P. R. Christensen^{98,44}, S. Church¹¹¹, D. L. Clements⁶⁷, S. Colombi^{72,116}, L. P. L. Colombo^{27,80}, C. Combet⁸⁹, A. Coulais⁸⁶, B. P. Crill^{80,14}, A. Curto^{78,7,83}, F. Cuttaia⁵⁷, L. Danese¹⁰³, R. D. Davies⁸¹, R. J. Davis⁸¹, P. de Bernardis⁴⁰, A. de Rosa⁵⁷, G. de Zotti^{54,103}, J. Delabrouille¹, F.-X. Désert⁶⁴, E. Di Valentino^{72,107}, C. Dickinson⁸¹, J. M. Diego⁷⁸, K. Dolag^{119,94}, H. Dole^{71,70}, S. Donzelli⁵⁸, O. Doré^{80,14}, M. Douspis⁷¹, A. Ducout^{72,67}, J. Dunkley¹¹², X. Dupac⁴⁷, G. Efstathiou^{75,83,*}, F. Elsner^{29,72,116}, T. A. Enßlin⁹⁴, H. K. Eriksen⁷⁶, M. Farhang^{11,102}, J. Fergusson¹⁵, F. Finelli^{57,59}, O. Forni^{117,12}, M. Frailis⁵⁶, A. A. Fraisse³³, E. Franceschi⁵⁷, A. Frejsel⁹⁸, S. Galeotta⁵⁶, S. Galli⁸², K. Ganga¹, C. Gauthier^{1,93}, M. Gerbino^{114,100,40}, T. Ghosh⁷¹, M. Giard^{117,12}, Y. Giraud-Héraud¹, E. Giusarma⁴⁰, E. Gjerløw⁷⁶, J. González-Nuevo^{23,78}, K. M. Górski^{80,123}, S. Gratton^{83,75}, A. Gregorio^{42,56,63}, A. Gruppuso⁵⁷, J. E. Gudmundsson^{114,100,33}, J. Hamann^{115,113}, F. K. Hansen⁷⁶, D. Hanson^{95,80,11}, D. L. Harrison^{75,83}, G. Helou¹⁴, S. Henrot-Versillé⁸⁵, C. Hernández-Monteagudo^{16,94}, D. Herranz⁷⁸, S. R. Hildebrandt^{80,14}, E. Hivon^{72,116}, M. Hobson⁷, W. A. Holmes⁸⁰, A. Hornstrup²⁰, W. Hovest⁹⁴, Z. Huang¹¹, K. M. Huffenberger³¹, G. Hurier⁷¹, A. H. Jaffe⁶⁷, T. R. Jaffe^{117,12}, E. Keihänen³², R. Keskitalo¹⁷, T. S. Kisner⁹¹, R. Kneissl^{46,9}, J. Knoche⁹⁴, L. Knox³⁵, M. Kunz^{21,71}, A. Lähteenmäki^{2,52}, J.-M. Lamarre⁸⁶, A. Lasenby^{7,83}, M. Lattanzi^{39,60}, C. R. Lawrence^{117,12}, F. Levrier⁸⁶, A. Lewis³⁰, M. Liguori^{38,79}, P. B. Lilje⁷⁶, M. Linden-Vørnle²², G. Maggio⁵⁶, D. Maino^{41,58}, N. Mandolesi^{57,39}, A. M...^{65,78}, S. M...⁴⁰, S. M...⁴⁰

Noncovalent Functionalization of Graphene and Graphene Oxide for Energy Materials, Biosensing, Catalytic, and Biomedical Applications

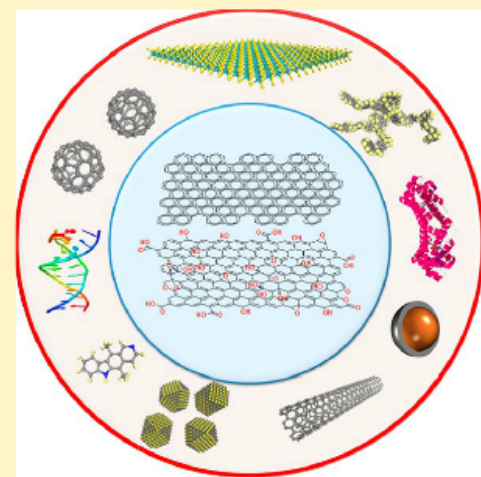
Vasilios Georgakilas,[†] Jitendra N. Tiwari,[‡] K. Christian Kemp,^{‡,||} Jason A. Perman,[§]
Athanasios B. Bourlinos,[§] Kwang S. Kim,^{*,‡} and Radek Zboril^{*,§}

[†]Material Science Department, University of Patras, 26504 Rio Patras, Greece

[‡]Center for Superfunctional Materials, Department of Chemistry, Ulsan National Institute of Science and Technology (UNIST), Ulsan 689-798, Korea

[§]Regional Centre of Advanced Technologies and Materials, Department of Physical Chemistry, Faculty of Science, Palacky University in Olomouc, 17 Listopadu 1192/12, 771 46 Olomouc, Czech Republic

ABSTRACT: This Review focuses on noncovalent functionalization of graphene and graphene oxide with various species involving biomolecules, polymers, drugs, metals and metal oxide-based nanoparticles, quantum dots, magnetic nanostructures, other carbon allotropes (fullerenes, nanodiamonds, and carbon nanotubes), and graphene analogues (MoS₂, WS₂). A brief description of π - π interactions, van der Waals forces, ionic interactions, and hydrogen bonding allowing noncovalent modification of graphene and graphene oxide is first given. The main part of this Review is devoted to tailored functionalization for applications in drug delivery, energy materials, solar cells, water splitting, biosensing, bioimaging, environmental, catalytic, photocatalytic, and biomedical technologies. A significant part of this Review explores the possibilities of graphene/graphene oxide-based 3D superstructures and their use in lithium-ion batteries. This Review ends with a look at challenges and future prospects of noncovalently modified graphene and graphene oxide.





Observation of Gravitational Waves from a Binary Black Hole Merger

B. P. Abbott *et al.**

(LIGO Scientific Collaboration and Virgo Collaboration)

(Received 21 January 2016; published 11 February 2016)

On September 14, 2015 at 09:50:45 UTC the two detectors of the Laser Interferometer Gravitational-Wave Observatory simultaneously observed a transient gravitational-wave signal. The signal sweeps upwards in frequency from 35 to 250 Hz with a peak gravitational-wave strain of 1.0×10^{-21} . It matches the waveform predicted by general relativity for the inspiral and merger of a pair of black holes and the ringdown of the resulting single black hole. The signal was observed with a matched-filter signal-to-noise ratio of 24 and a false alarm rate estimated to be less than 1 event per 203 000 years, equivalent to a significance greater than 5.1σ . The source lies at a luminosity distance of 410_{-180}^{+160} Mpc corresponding to a redshift $z = 0.09_{-0.04}^{+0.03}$. In the source frame, the initial black hole masses are $36_{-4}^{+5} M_{\odot}$ and $29_{-4}^{+4} M_{\odot}$, and the final black hole mass is $62_{-4}^{+4} M_{\odot}$, with $3.0_{-0.5}^{+0.5} M_{\odot} c^2$ radiated in gravitational waves. All uncertainties define 90% credible intervals. These observations demonstrate the existence of binary stellar-mass black hole systems. This is the first direct detection of gravitational waves and the first observation of a binary black hole merger.

DOI: [10.1103/PhysRevLett.116.061102](https://doi.org/10.1103/PhysRevLett.116.061102)

I. INTRODUCTION

A 2.2 μW , -12 dBm RF-Powered Wireless Current Sensing Readout Interface IC With Injection-Locking Clock Generation

Fu-To Lin, *Student Member, IEEE*, Shao-Yung Lu, *Student Member, IEEE*, and Yu-Te Liao, *Member, IEEE*

Abstract—This paper presents a wireless-powering current-sensing readout system on a CMOS platform for portable electrochemical measurement. The wireless sensing system includes energy-efficient power management circuitry, a sensor readout interface, and a backscattering wireless communication scheme. For power-and-area-constrained bio-sensing applications, the proposed readout circuitry incorporates an ultra-low-power potentiostatic system that generates a current according to the electrochemical reaction, as well as an oscillator-based time-to-digital converter instead of a voltage-domain analog-to-digital converter. To avoid a bulky battery and power-hungry clock reference, the chip is wirelessly powered and injection-locked by the modulated radio waves, which includes a 918 MHz carrier signal mixed with a 3.2 MHz modulated signal. The chip, implemented using a 0.18- μm CMOS process, occupies a silicon area of 1 mm². The proposed design achieves a sensitivity of 289 Hz/nA and a current range of 200

a point of care, these devices need to be capable of portable biomedical analysis at a low cost. With the advent of CMOS technology, an electrochemical sensor array can be integrated on a single silicon chip [4] for bio-implants and wearables. The dense sensing array, small form factor, and reduced long external connections of these microsystems extend the limit of detection resolution by improving the signal-to-noise ratio and reducing environmental interference coupling. The development of a CMOS-based electrochemical platform would enable a new breed of highly versatile portable electrochemical applications. However, the development of portable electrochemical



Contents lists available at ScienceDirect

Physics Letters B

www.elsevier.com/locate/physletb



750 GeV diphoton resonance, 125 GeV Higgs and muon $g - 2$ anomaly in deflected anomaly mediation SUSY breaking scenarios



Fei Wang^{a,b,*}, Lei Wu^c, Jin Min Yang^{b,d}, Mengchao Zhang^b

^a School of Physics, Zhengzhou University, Zhengzhou 450000, China

^b Key Laboratory of Theoretical Physics, Institute of Theoretical Physics, Academia Sinica, Beijing 100190, China

^c ARC Centre of Excellence for Particle Physics at the Terascale, School of Physics, The University of Sydney, NSW 2006, Australia

^d Department of Physics, Tohoku University, Sendai 980-8578, Japan

ARTICLE INFO

Article history:

Received 22 March 2016

Received in revised form 4 May 2016

Accepted 21 May 2016

Available online 25 May 2016

Editor: G.F. Giudice

ABSTRACT

We propose to interpret the 750 GeV diphoton excess in deflected anomaly mediation supersymmetry breaking scenarios, which can naturally predict couplings between a singlet field and vector-like messengers. The CP-even scalar component (S) of the singlet field can serve as the 750 GeV resonance. The messenger scale, which is of order the gravitino scale, can be as high as 10^5 GeV. The messenger species N_F and the deflection parameter d can be chosen to accommodate the 125 GeV Higgs boson and the muon $g - 2$ anomaly, without conflicting with the LHC constraints. The deflection parameter d can be chosen to accommodate the 750 GeV diphoton resonance in anomaly mediation supersymmetry breaking scenarios.

© 2016 Elsevier B.V.

A lithium–oxygen battery based on lithium superoxide

Jun Lu^{1*}, Yun Jung Lee^{2*}, Xiangyi Luo^{3,4*}, Kah Chun Lau^{3*}, Mohammad Asadi^{5*}, Hsien-Hau Wang³, Scott Brombosz³, Jianguo Wen⁶, Dengyun Zhai¹, Zonghai Chen¹, Dean J. Miller⁶, Yo Sub Jeong², Jin-Bum Park², Zhigang Zak Fang⁴, Bijandra Kumar⁷, Amin Salehi-Khojin⁵, Yang-Kook Sun², Larry A. Curtiss³ & Khalil Amine¹

Batteries based on sodium superoxide and on potassium superoxide have recently been reported^{1–3}. However, there have been no reports of a battery based on lithium superoxide (LiO₂), despite much research^{4–8} into the lithium–oxygen (Li–O₂) battery because of its potential high energy density. Several studies^{9–16} of Li–O₂ batteries have found evidence of LiO₂ being formed as one component of the discharge product along with lithium peroxide (Li₂O₂). In addition, theoretical calculations have indicated that some forms of LiO₂ may have a long lifetime¹⁷. These studies also suggest that it might be possible to form LiO₂ alone for use in a battery. However, solid LiO₂ has been difficult to synthesize in pure form¹⁸ because it is thermodynamically unstable with respect to disproportionation, giving Li₂O₂ (refs 19, 20). Here we show that crystalline LiO₂ can be stabilized in a Li–O₂ battery by using a suitable graphene-based cathode. Various characterization techniques reveal no evidence of Li₂O₂. A novel templating growth

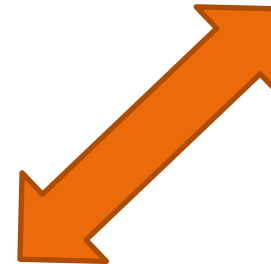
electrolyte (1 M LiCF₃SO₃ in tetraethylene glycol dimethyl ether (TEGDME)) impregnated into a glass fibre separator, and a porous cathode. A current density of 100 mA g⁻¹ was used for both discharge and charge, and the cell was run with a capacity limit of 1,000 mA h g⁻¹ to avoid side reactions. The specific capacity (mA h g⁻¹) and the current density (mA g⁻¹) are based on the active materials of the O₂ electrodes. Figure 2a and b shows voltage profiles for the Ir–rGO and rGO cathode architectures, respectively. The Ir–rGO discharge product shows a very low charge potential of ~3.2 V that rises to 3.5 V over 40 cycles leading to more than 85% efficiency in this system (Fig. 2a). The voltage profile of the rGO cathode shows a low charge potential of ~4.2 V with a low

The discharge and charge profiles of the Ir–rGO and rGO cathodes are shown in Figure 2a and b, respectively. The Ir–rGO cathode shows a very low charge potential of ~3.2 V that rises to 3.5 V over 40 cycles leading to more than 85% efficiency in this system (Fig. 2a). The voltage profile of the rGO cathode shows a low charge potential of ~4.2 V with a low

Woran erkennt man das?



Autoren



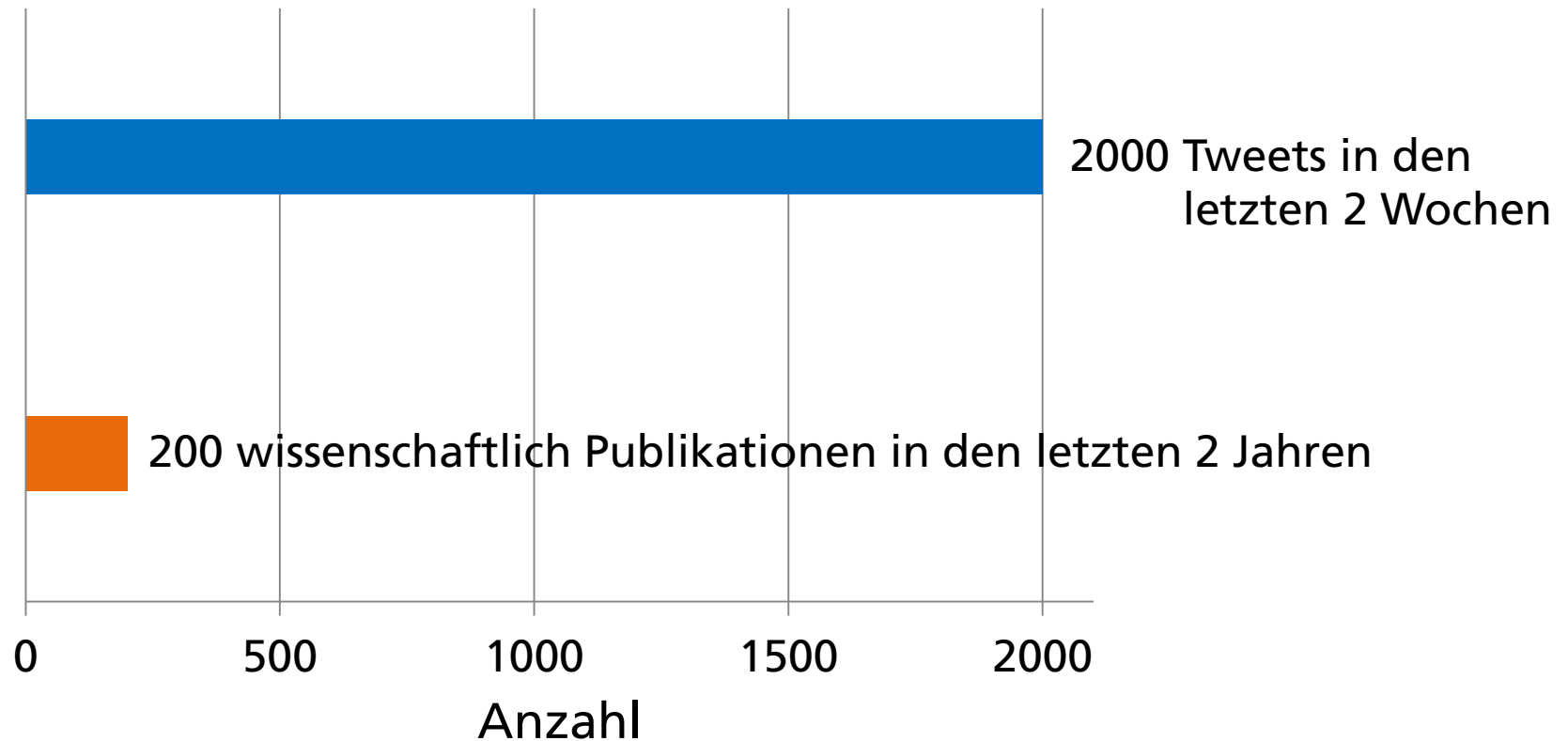


Kann man **das** dem Computer bei bringen?

Cognitive Computing

in der Zukunftsforschung

Cognitive Computing – it's a Buzzword



IBM Watson siegt mit der
Technologie des *Cognitive*
Computing bei Jeopardy!

Cognitive Computing ist ...

.... ein Sammelsurium von Technologien

- Computer Linguistik
- Content Analytics



Inhalte, Kontext und
Bedeutung analysieren

- Suchfunktionalität
für große Text-
und Datenmengen



Leistungsfähige,
konfigurierbare Suche

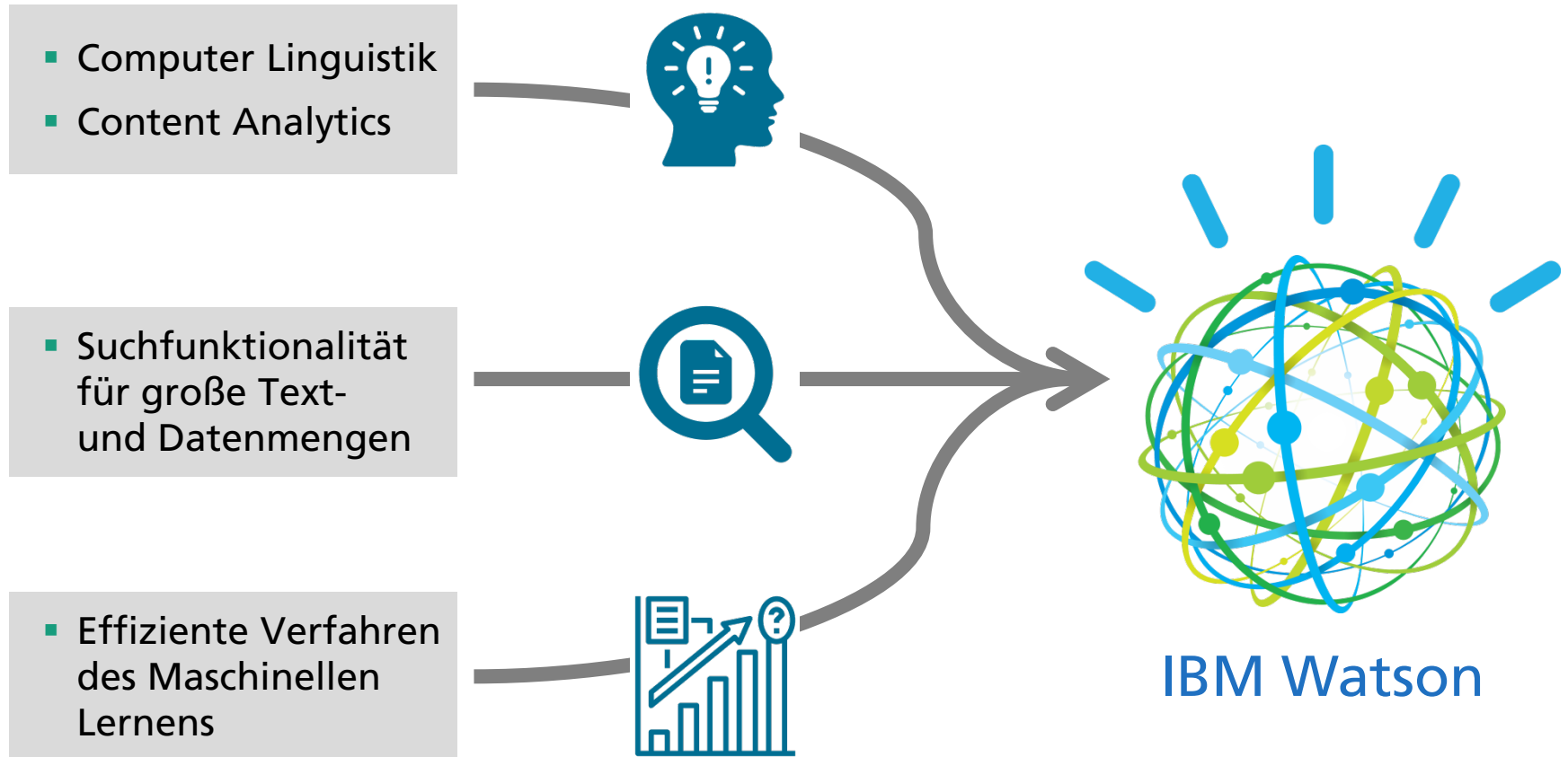
- Effiziente Verfahren
des Maschinellen
Lernens



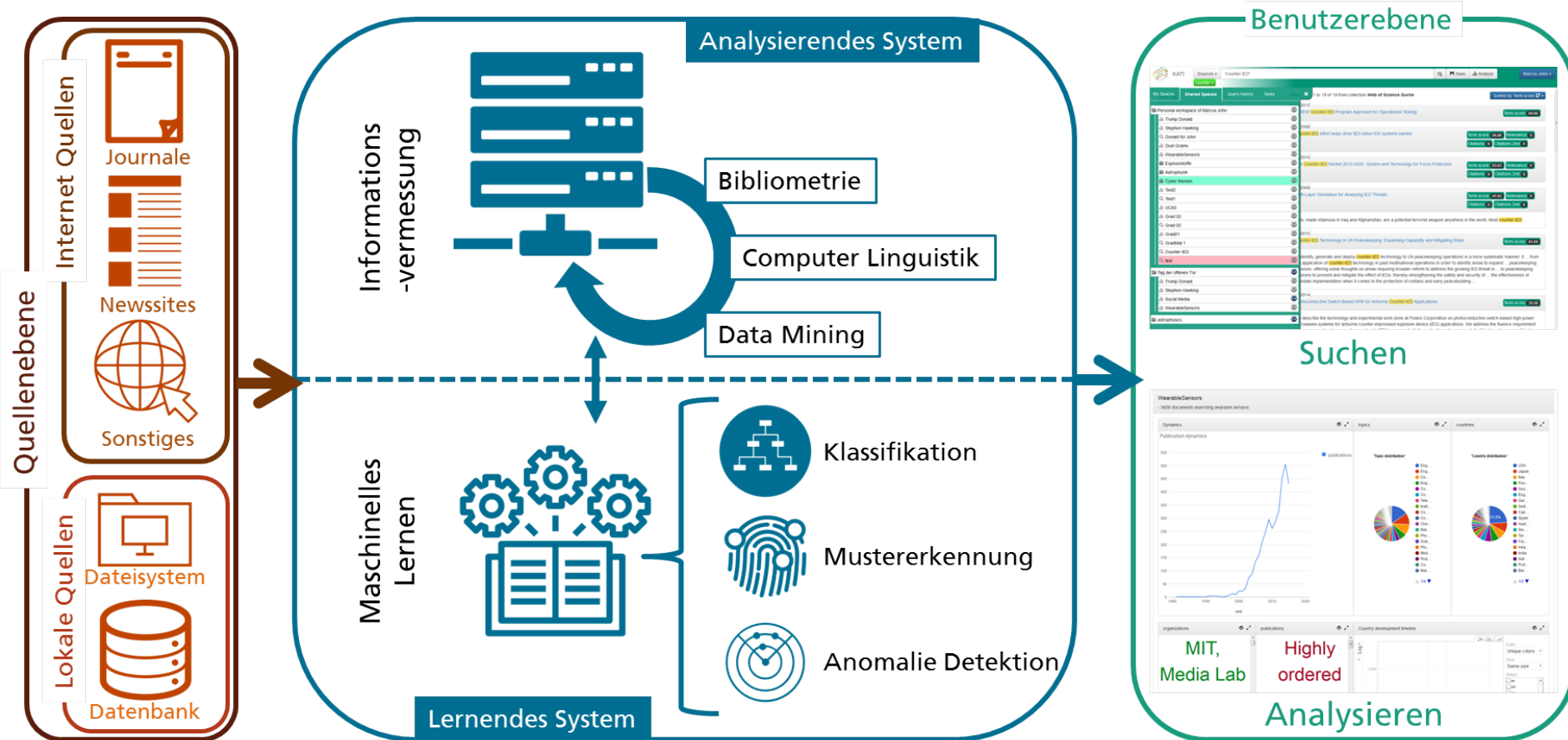
- Muster erkennen
- Hypothesen generieren
- **Vorhersagen machen**

Cognitive Computing ist ...

... ein Softwarepaket von IBM!



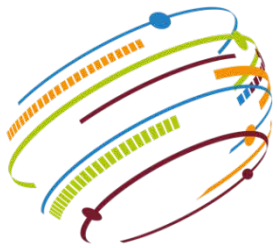
Unser Ansatz



Aus

IBM Watson


... wird KATI




Knowledge Analytics for Technology & Innovation
with Watson


Wo stehen wir heute?


Planung & Aufbau
der Hardware 


Software installiert 

Datenmodell entworfen
und Datenbank befüllt 


50.542.097 Datensätze des Web of Science
in die Watson Maschine importiert 


Visualisierungen programmieren 

Schnittstellen implementiert 

Anwendungsfälle realisiert 

Inhalt des Web of Science
erschlossen 

Weitere Quellen erschließen 

Es gib noch viel zu tun 

Suchoberfläche

KATI Sources "donald trump" Save Analyze Marcus John

trump

Primary Author (10)

date (10)

manual Tag (8)

WoS Categories (10)

organization (7)

Research Area (8)

Country (2)

publisher (8)

Author (10)

language (1)

source (2)

abstract (1)

Documents 1 to 16 of 16 from collection WOS

19.10.2015
WHAT'S **DONALD TRUMP** REALLY WORTH?

01.10.2015
Donald Trump's America

22.07.1996
Donald Trump: An ex-loser is back in the money

01.09.2015
Mediacracy Making Use of **Donald Trump**

14.10.2010
Save **Donald Trump!** Is now a really bad time to

15.02.2005
No such thing as over-exposure: Inside the life

17.11.2008
Problem Loan

Trouble for **Donald Trump**: The money for a condo

01.09.2015
This 22-Year-Old Really, Really, Really Wants

23.05.2011
What's in Your Wallet?

Donald Trump, flirting with a presidential run, ins

Sorted by Term score Next

Problem Loan

17.11.2008
by Randall, David K.

article publication

Term score: 83.54

Abstract

Trouble for Donald Trump: The money for a condo project didn't come through

Properties

Times cited	0
Times cited (2nd degree)	0
Relevance score	0
accession number	368WC
address count	0
author count	1
from year	2008
number of grants	0
has author	Randall, David K.
has date	2008-11-17T00:00:00Z
has source	WOS.SSCI
has topic	Business, Finance Business & Economics

Analyseoberfläche

WearableSensors

- 3608 documents searching wearable sensors

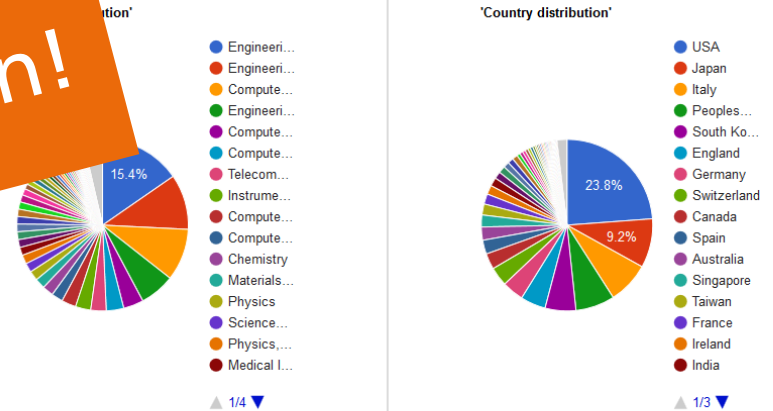
Dynamics

Publication dynamics



Eine
Demonstration
gibt es im Raum Bonn!

countries



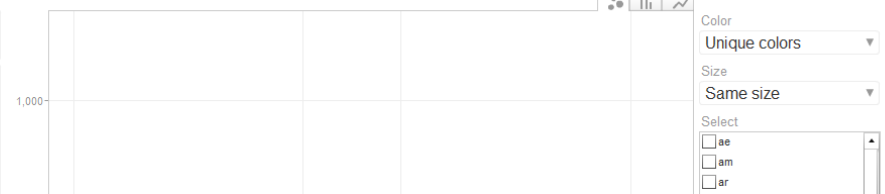
organizations

MIT, Media Lab
Natl Univ
Singapore, Dent

publications

Highly ordered
nanowire arrays

Country development timeline



An KATI beteiligte Personen

Gerald Walther Sabrina Müller
Matthias Grüne Michael Bach
Angela Haberlach Diana Freudendahl
Anna Julia Schulte Siegrid Hecht-Veenhuis Beate Becker
Christoph Schemaschek Silke Römer Line Kurka Andre Pichler
Frank Fritsche Ulrik Neupert Patrick Lieberz Isabelle Linde-Frech
Guido Huppertz Sylvia Scheid Rene Bantes Udo Rector Klaus Ruhlig
David Offenberg Matthias Grüne Prof. Lauster Rosemarie Engels
Ramona Langner Hans-Martin Pastuszka Carsten Heuer
Heike Brandt Monika Artz Stefan Reschke
Daniela Lieberz

Kontakt



Fraunhofer Institut für
Naturwissenschaftlich-Technische
Trendanalysen INT
Euskirchen, Germany

Dr. Marcus John

marcus.john@int.fraunhofer.de

